Ab Initio Topological Analysis of the Electronic Density in *n*-Butonium Cations and Their van der Waals Complexes

Nora B. Okulik,*,† Laura G. Sosa,‡ Pierre M. Esteves,§,|| Claudio J. A. Mota,§ Alicia H. Jubert,⊥ and Nélida M. Peruchena‡

Facultad de Agroindustrias, UNNE, Cte. Fernández 755, (3700) Pcia. R. Sáenz Peña, Chaco, Argentina, Area de Quimica Fisica, Deptartamento Química, Facultad Ciencias Exactas, Nat. y Agrim., UNNE., Av. Libertador 5300, (3400) Corrientes, Argentina, Instituto de Química, Departamento de Química Orgânica, Universidade Federal de Rio de Janeiro, Cidade Universitária CT Bloco A, 21949-900 Rio de Janeiro, Brasil, and CEQUINOR, Centro de Química Inorgánica (CONICET, UNLP), Departamento de Química, Facultad de Ciencias Exactas, UNLP, C. C. 962, (1900) La Plata, Argentina

Received: August 7, 2001; In Final Form: December 4, 2001

In this work, the topology of the ab initio electronic density charge, using the theory of atoms in molecules (AIM), developed by Bader, is studied for the *n*-$C_4H_{11}^+$ species, the protonated *n*-butane. The electronic delocalization that operates through the σ bonds in saturated molecules and specifically in protonated alkanes is studied by means of analysis of the charge density and the bond critical points. This analysis is used in order to establish a relationship among the parameters that determine the stability order found for the different species and relate them with the carbonium ions structure. Comparing these results with the *i*-$C_4H_{11}^+$ allow us to study the nature of the 3c−2e bonds in alkanes in greater detail, permitting the description on the σ basicity and reactivity scales in terms of structural parameters of the carbonium ions.

Introduction

Carbonium ions are important species involved in acid-catalyzed transformations. They are formed by the protonation of alkanes in liquid superacids, and there is evidence for the formation of pentacoordinated carbonium ions.[1−3] These species contain three-center two-electron bonds (3c−2e) and can be generated upon the insertion of a proton or carbenium ion into the C−H or C−C bonds.

Because of the shortage of direct experimental observation of carbonium ions, their structure and energy have been mostly studied by theoretical methods. The use of ab initio calculations, particularly those including electron correlation effects, has proven to provide excellent predictions for the energy and geometry of methonium (CH_5^+),[4−7] ethonium ($C_2H_7^+$),[8] proponium,[9] and isobutonium.[10,11] Esteves et al.[12] investigated the structure and energetics of the *n*-butonium cations (*n*-$C_4H_{11}^+$). Protonation of *n*-butane can take place at the primary C−H bonds (six overall), at the secondary C−H bonds (four overall), and at two distinct types of C−C bonds (two external and one internal) to form different isomeric structures of the *n*-$C_4H_{11}^+$ cation, as shown in Scheme 1.

The stability of the carbonium ions, formed by the protonation of the different σ bonds of *n*-butane, decreases in the order: 2-C-*n*-butonium > 1-C-*n*-butonium > 2-H-*n*-butonium > 1-H-*n*-butonium. The protonated butane species are isomeric to the isobutonium cations, which allows a direct energy comparison among the different $C_4H_{11}^+$ carbocations.

SCHEME 1: Nonequivalent Bonds in *n*-Butane Leading to the Different *n*-Butonium Ions by Hypothetical Protonation

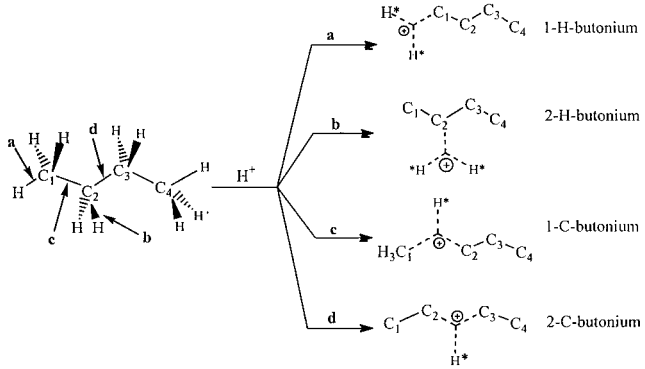

Olah and collaborators,[13] on the basis of the reactivity of several alkanes in liquid superacids, proposed a σ-reactivity scale, which follows the order

$$\textit{tert}\text{-C}-\text{H} > \text{C}-\text{C} > \textit{sec}\text{-C}-\text{H} > \textit{prim}\text{-C}-\text{H} > \text{CH}_4$$

Esteves et al.,[12] comparing the relative stability of the several $C_4H_{11}^+$ isomers, proposed the following σ-basicity scale:

$$\text{C}-\text{C} > \textit{tert}\text{-C}-\text{H} > \textit{sec}\text{-C}-\text{H} > \textit{prim}\text{-C}-\text{H} > \text{CH}_4$$

This scale differs slightly from the one proposed by Olah, because they do not correspond to the same phenomena. Olah's scale is related to the reactivity of the σ bond, which is a kinetic property, whereas Esteves' scale is based on relative stability, reflecting the basicity of the system. The later is related with thermodynamics of the protonation of the σ bonds.

* To whom correspondence should be addressed.
† Facultad de Agroindustrias, UNNE.
‡ Facultad Ciencias Exactas, Nat. y Agrim., UNNE.
§ Universidade Federal de Rio de Janeiro.
|| Present Address: Loker Hydrocarbon Research Institute, University of Southern California, Los Angeles, California 90089-1661.
⊥ Facultad de Ciencias Exactas, UNLP.

10.1021/jp0130665 CCC: $22.00
Published on Web 02/02/2002

Further studies[14] involving explicitly the anion and solvation of superacid models confirm the reactivity nature of Olah's scale.[13]

The theory of atoms in molecules (AIM), developed by Bader,[15,16] is a simple, rigorous, and elegant way of defining atoms, bonds, and chemical structure. This theory is based on the critical points (CP) of the electronic density distribution, $\rho(\mathbf{r})$. These are points where the electronic density gradient, $\nabla\rho(\mathbf{r})$, vanishes and are characterized by the three eigenvalues (λ_1, λ_2, λ_3) of the Hessian matrix of $\rho(\mathbf{r})$. The CP are labeled as (r, s) according to their rank, r (number of nonzero eigenvalues), and signature, s (the algebraic sum of the signs of the eigenvalues).

Four types of CP are of interest in molecules: (3, −3), (3, −1), (3, +1), and (3, +3). A (3, −3) point corresponds to a maximum in $\rho(\mathbf{r})$, characterized by $\nabla^2\rho(\mathbf{r}) < 0$, and occurs generally at the nuclear positions. A (3, +3) point indicates electronic charge depletion, and it is characterized by $\nabla^2\rho(\mathbf{r}) > 0$. It is also known as box critical point. (3, +1) points, or ring critical points, are saddle points. Finally, a (3, −1) point, or bond critical point (BCP), is generally found between two neighboring nuclei indicating the existence of a bond between them.

Several properties that can be evaluated at the BCP constitute very powerful tools to classify the interactions between two fragments.[17−18] The two negative eigenvalues of the Hessian matrix (λ_1 and λ_2) measure the degree of contraction of ρ_b perpendicular to the bond toward the critical point, whereas the positive eigenvalue (λ_3) measures the degree of contraction parallel to the bond and from the BCP toward each of the neighboring nuclei. When the negative eigenvalues dominate, the electronic charge is locally concentrated within the region of the BCP leading to an interaction characteristic of covalent or polarized bonds and being characterized by large ρ_b values, $\nabla^2\rho_b < 0$, $|\lambda_1|/\lambda_3 > 1$, and $G_b/\rho_b < 1$, being G_b the local kinetic energy density at the bond critical point. If the positive eigenvalue is dominant, on the other hand, the electronic density is locally concentrated at each atomic site. The interaction is now referred to as a closed-shell one, and it is characteristic of highly ionic bonds, hydrogen bonds, and van der Waals interactions. It is characterized by relatively low ρ_b values, $\nabla^2\rho_b > 0$, $|\lambda_1|/\lambda_3 < 1$, and $G_b/\rho_b > 1$. Finally, the ellipticity, ϵ, defined as $\lambda_1/\lambda_2 - 1$ indicates the deviation of the electronic charge density from the axial symmetry of a chemical bond providing a quantitative measure of the π character of the bond or of the delocalization electronic charge.

Application of this theory to understand the nature of the 3c−2e bonds in carbonium ions in deeper detail is an interesting approach and has been performed by our group for other carbonium ion structures.[19]

In this work, the topology of the electronic density charge is studied for *n*-$C_4H_{11}^+$ species, at ab initio level using the AIM theory developed by Bader.[14,15] The electronic delocalization that operates through the σ bonds in saturated molecules and specifically in protonated alkanes can be studied by means of analysis of the charge density and the bond critical points. This analysis will be used in order to establish a relationship among the parameters that determine the stability order found for the different species and relate them with the carbonium ions structure. Comparing these results with the *i*-$C_4H_{11}^+$ allows us to study the nature of the 3c−2e bonds in alkanes in greater detail, permitting the description on the σ basicity and reactivity scales in terms of structural parameters of the carbonium ions.

Method and Calculation Details

Calculations, at Hartree−Fock single reference second and fourth order Møller−Plesset perturbation theory (MP2 and MP4), were performed for the *n*-butonium cations and their van der Waals complexes (Figure 1). The geometries of all of the species were fully optimized. These systems are confirmed as true minima in the potential energy surface by the presence of only real harmonic frequencies after the corresponding vibrational analysis. Calculations were carried out at the MP4SDTQ(fc)/6-311+G**//MP2(full)/6-31G** level. All these calculations were performed using the Gaussian 94 package.[20]

The topological analysis and the evaluation of local properties are accomplished by means of the PROAIM program,[21] using wave functions obtained at the RHF level of theory and the 6-311++G** basis set provided by the Gaussian 94 package.[20] Topological calculations performed at the MP2/6-311++G** level showed no significant differences with results obtained at the HF/6-311++G** level.[19b]

Figure 1 shows the 15 structures that were located as minima in the potential energy surface. Protonation at the primary C−H bond produces structures **1**−**3**, corresponding to conformational isomers of the 1-H-*n*-butonium cation. Protonation of the secondary C−H bonds leads to structures **4**−**6**, the conformer of the 2-H-*n*-butonium cation. Protonation at primary C−C bonds (external) forms the conformers **7**−**9**, corresponding to the 1-C-*n*-butonium ion, and protonation at the secondary C−C bond (internal) leads to the conformers **10**−**11** of the 2-C-*n*-butonium cation. Other minima in the PES were also found, and they correspond to van der Waals complexes. Structure **12** corresponds to the complex between the *sec*-butyl cation and H_2. Structure **13** represents the $C_2H_5^+$ cation plus ethane. The complex between protonated methylcyclopropane plus hydrogen corresponds to structure **14**, whereas protonated cyclopropane plus methane is shown as structures **15**. The stability of the de van der Waals complexes decreased in the order **12** > **15** > **14** > **13**.[12]

Results and Discussion:

***n*-$C_4H_{11}^+$ Cations.** Table 1 shows the most significant topological local properties at the bond critical points (3, −1) for structures **1**−**3** corresponding to the 1-H-*n*-butonium cations. We have also included the bond distances and other relevant properties for 1-H-isobutonium, **3′**, for comparison purposes. The topological local properties reported correspond to the bond critical points from C−H*, H*−H*, C−C, C−H_0, and C−H'_0, where H* represents the hydrogen atom involved in the 3c−2e bond and H_0 and H'_0 correspond to the other H atoms located on the C_1 atom (see Figure 1).

The comparative analysis on the BCP of the C−H* vs C−H_0 bonds allow us to make the following comments: In the 1-H-*n*-butonium cations, the electronic density (ρ) and the Laplacian of the density ($\nabla^2\rho$) values in the BCP at the C−H bonds are smaller than those at the C−H_0 bonds, whereas the relationship between the perpendicular and parallel curvature of the bond trajectory, $|\lambda_1|/\lambda_3$, is notably higher in the C−H* bonds than in the C−H_o ones. Regarding the energy densities, at BCP, it can be seen that the potential energy density value, V_b, does not show remarkably differences between both types of bonds. Notwithstanding, the kinetic energy density values, G_b, in the C−H* are remarkably greater than those on the C−H_0 taken as reference. As a consequence of what was pointed out above, dramatic differences on the kinetic energy density per charge unit G_b/ρ_b and on the relationship V_b/G_b are found. Thus, G_b/ρ_b is four times higher, whereas V_b/G_b is three times smaller on

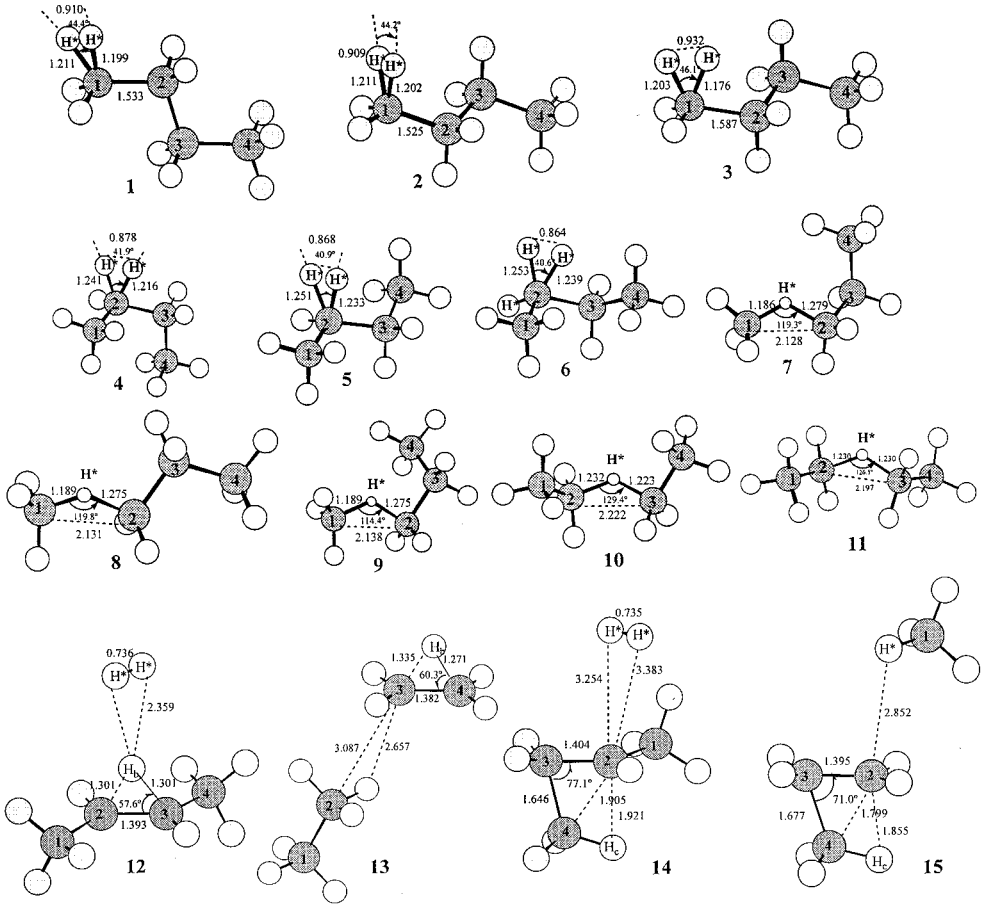

Figure 1. Geometries of *n*-$C_4H_{11}^+$ carbocations and van der Waals complexes at MP4SDTQ(fc)/6-311+G/MP2(full)/6-31G** level. (a) Structures **1**−**11** and (b) structures of van der Waals complexes **12**−**15**.

TABLE 1: Topological Properties (in a.u.) of the Electronic Charge Density in 3c−2e BCP and Their Neighbor Bonds of 1-H-*n*-Butonium Cations (1−3; see Figure 1)[a]

		d(C−H*)	angle H*-C−H*	ρ_b	$\nabla^2\rho_b$	$\lvert\lambda_1\rvert/\lambda_3$	ϵ	G_b	V_b	G_b/ρ_b	V_b/G_b
1	C_1−H*	1.211	44.4	0.2128	−0.4145	4.6723	1.6686	0.1296	−0.3630	0.6090	2.8009
	C_1−H*	1.199									
2	C_1−H*	1.211	44.2	0.2122	−0.4070	4.6145	1.7959	0.1303	−0.3624	0.6140	2.7813
	C_1−H*	1.202									
3	C_1−H*	1.203	46.1	0.2200	−0.4744	9.4066	5.5505	0.0892	−0.2970	0.4055	3.3296
	C_1−H*	1.176									
3′	C_1−H*	1.217	43.7	0.2090	−0.3783	3.8933	1.6170	0.1358	−0.3661	0.6498	2.6959
	C_1−H*										
1	H*−H*	0.910		0.2195	−0.5816	2.9599	1.5809	0.0388	−0.2240	0.1768	5.7732
2		0.909		0.2197	−0.5854	3.0005	1.5834	0.0388	−0.2239	0.1766	5.7706
3		0.932		0.2204	−0.5322	7.0232	4.5417	0.0511	−0.2352	0.2319	4.6027
3′		0.903		0.2200	−0.6002	2.8654	1.3855	0.0364	−0.2229	0.1655	6.1236
1	C_1−C_2	1.533		0.2376	−0.6373	2.1332	0.0178	0.0771	−0.3134	0.3245	4.0649
2		1.525		0.2433	−0.6661	2.2106	0.0224	0.0783	−0.3232	0.3218	4.1277
3		1.587		0.2069	−0.4704	1.6968	0.0751	0.0672	−0.2520	0.3230	4.8065
1	C_1−H_0	1.101		0.2749	−0.9777	1.5700	0.0010	0.0347	−0.3139	0.1262	9.0461
2		1.102		0.2746	−0.9755	1.5746	0.0183	0.0347	−0.3132	0.1264	9.0259
3		1.084		0.2922	−1.0987	1.6177	0.0311	0.0304	−0.3355	0.1117	11.0362
1	C_1−H'_0	1.087		0.2910	−1.0925	1.6069	0.0325	0.0295	−0.3322	0.1014	11.2610
2		1.089		0.2878	−1.0727	1.5966	0.0356	0.0298	−0.3276	0.1035	10.9933
3		1.084		0.2916	−1.0972	1.6148	0.0310	0.0300	−0.3343	0.1029	11.1433

[a] Also, some relevant properties for 1-H-*iso*-butonium (**3′**) are included. See the Method and Calculation Details section for an explanation of symbols. In all cases, (*) indicates the hydrogen atom involved in the 3c-2e bond and (0) indicates the hydrogen atom taken as reference. Bond distances in angstroms and angles in degrees are included.

the C−H* than on the C−H_0 ones. It has to be mentioned that the kinetic and potential energy density values for a covalent bond in a normal hydrocarbon show a difference close to 1 order of magnitude, with a V_b/G_b relationship between **5** (in C−C) and **10** (in C−H). It can be noticed that in the covalent C−H* bonds that participate in the three center bond in this relationship

SCHEME 2: Interconversion, Bond-to-Bond Rearrangement, of H-Carbonium to C-Carbonium Ion as a Possible Pathway to Explain Products of C−C Protonation in Superacid Catalyzed Alkane Reactions

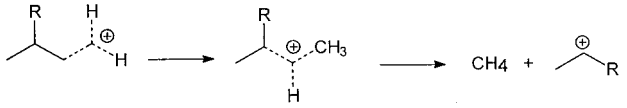

has a much smaller value (2.80, 2.78, and 3.33). These findings clearly show that the interaction among the pentacoordinated C and the H* atoms is of a covalent type but weaker than a C−H bond in *n*-alkanes. The topological properties on the C_1-C_2 BCP do not show remarkable differences with the C−C bond of *n*-butane.[15]

Analysis of the topological properties corresponding to the H*−H* BCP of the different structures shows that ρ_b and $\nabla^2\rho_b$ values are smaller than those in the isolated H_2 molecule (ρ_b = 0.2671 au and $\nabla^2\rho_b = -1.1279$ au, at the same level of calculation). A dramatic change in the ellipticity value is also observed (from 0.0 in the isolated H_2 molecule to 1.58, 1.58, and 4.54 for the species **1**, **2**, and **3**, respectively). The abnormally high ellipticity value, at H−H* BCP, for the structure **3,** as well as the high value of the $|\lambda_1|/\lambda_3$ relationship indicate that the (3, −1) BCP is close to a degeneracy ($\lambda_1 = -0.5127$, $\lambda_2 = -0.0925$, $\lambda_3 = 0.0730$). The two last values are approximately zero and are indicative of the proximity of a structural change, possibly a rearrangement. H-carbonium ions are believed to undergo easy "bond-to-bond" (isotopal) rearrangement (see Scheme 2),[22,11] which seems to be supported by the present finding. It has to be pointed out that the fact that the λ_2 and λ_3 eigenvalues are close to zero implies that the CP is close to a degeneracy. In the AIM theory, the theorem of structural stability of Palis and Smale[23] is adopted to describe the structural changes in a molecular system. According to this theorem, one of the conditions that determines that a nuclear configuration is structurally stable is the existence of a number of finite non degenerated CPs.

In addition, the set of BCPs defines the network of bond paths and describes the molecular structure. The molecular graphs, formed by the network of these bond paths or trajectories, corresponding to all species are shown in Figure 2. A bent bond between the two H* atoms with a significant difference between the trajectory and the length of the bond can be seen (Δd = 0.187, 0.183, and 0.306 Å for structures **1**, **2**, and **3**, respectively). This indicates a high polarization of the H−H bond, bending the electronic density of this bond, by the interaction with the primary carbenium ion, as indicated by the resonance structure III in Scheme 3. Another picture would be the polarization of the C−H bond by the interacting H^+ in resonance structures I and II (Scheme 3).

In Table 2 are shown the topological properties on the bond critical points from the 3c−2e and neighbor bonds from the 2-H-*n*-butonium cations (structures **4**, **5**, and **6**) and 2-H-isobutonium cation, **6′**, for comparison purposes. For the species **4**, **5**, and **6**, where the protonation occur on the C−H secondary bond, we found that the density and Laplacian values on the C−H* BCP are smaller than those corresponding to the 1-H-*n*-butonium species. It has to be pointed out that the $C-C_{ethyl}$ bond results are 0.044, 0.009 and 0.013 Å larger than the secondary C−C bond in the normal *n*-butane. These results are consistent with the density and Laplacian values for these bonds.

It is interesting to note that in the 2-H-*n*-butonium cations the slightly higher values of the density and Laplacian of the H*−H* BCPs indicate that the interaction between these two nuclei is stronger than that observed in the 1-H-*n*-butonium cations. The same trend is reflected in the low ellipticity values, showing a less perturbed H_2 molecule participating in the 3c−2e bond. These results can be associated to a more stable secondary carbenium ion in the resonance structure III (Scheme 3), which increases its contribution in the description of the 3c−2e bond. The molecular graphs corresponding to these structures are similar to the 1-H-*n*-butonium ions. Differences of 0.113, 0.0942, and 0.0892 Å for the species **4**, **5**, and **6** are found between the trajectories and geometric distances of the bonds, being smaller than the equivalent ones calculated the 1-H-*n*-butonium cations.

Table 3 summarizes the main topological properties on the BCP corresponding to the 3c−2e bonds and their neighbor bonds in the C-*n*-butonium cations (structures **7**−**11**) and some relevant properties in the C-*iso*-butonium cation (**11′**). The first three entries of the table correspond to structures **7**−**9**, where the protonation is produced on the terminal C−C bond (1-C-*n*-butonium cations). The topological distribution of the electronic charge density in the cations **7**−**9** are very similar among them.

Analysis of local properties at the BCP of the C−H* and $C-H_0$ bonds shows that all of these bonds can be characterized as covalent bonds or shared interactions. Nevertheless, they show significative differences: the electronic density (ρ_b) and the Laplacian of the density ($\nabla^2\rho_b$) values in the BCPs at the C−H* bonds in the 3c−2e bonds are lower than those at the $C-H_0$ bonds, indicating a covalent weakened interaction. On the other hand, the elipticities of these bonds are significantly higher (0.1731 au at C−H* bond vs 0.0292 au at C_1-H bond in structure 7) than the values found for the parent H-carbonium ions. These observations are in agreement with a delocalization of electron charge density.

These results also show that the kinetic energy density values, G_b, and the potential energy density, V_b, at the C−H* bonds are greater and lower, respectively, than the same properties at the $C-H_0$ taken as reference. As a consequence of what was pointed out above, differences on the kinetic energy density per charge unit, G_b/ρ_b, and on the relationship V_b/G_b are found.

The topological distribution of the charge density at the three-center region in $C_{prim}-H^*$ and $C_{sec}-H^*$ bonds (i.e., in structure 7) can be compared against the values found in *n*-butane: 0.1908 and 0.1413 au and 0.2809 and 0.2814 a.u, respectively, for the carbonium ion and butane.

The facts previously remarked clearly show that the interaction at the 3c−2e bond, C−H*−C, is different to the interaction found in a C−H bond in an alkane.

Besides, the topological properties at BCPs on the C_1-C_2 bonds (structures **9**−**11**) also show some differences with the typical C−C bond from a normal hydrocarbon (at $C_{prim}-C_{sec}$ and $C_{sec}-C_{sec}$ in *n*-butane the values are ρ_b = 0.2556 and 0.2577 u.a.; $\nabla^2\rho_b = -0.6900$ and -0.6982 au; ϵ = 0.0074 and 0.0172 au; G_b= 0.0522 and 0.0528 au; $V_b = -0.2769$ and -0.2802 au, respectively).

Finally, in the **7**−**11** structures, the higher values of ρ_b, $\nabla^2\rho_b$, and ϵ at the BCPs in all of the C−C bonds are associated with a higher electronic charge delocalization over all of the network bonds in C-*n*-butonium cations.

Figure 3 shows the contour map of the Laplacian distribution $\nabla^2\rho$ for the structure **11**, in the plane that contains the 3c−2e bond. In this map, the shared interaction between C−H*−C atoms can be seen.

van der Waals Complexes. *van der Waals Complex **12***. Table 4 shows the more significant topological local properties

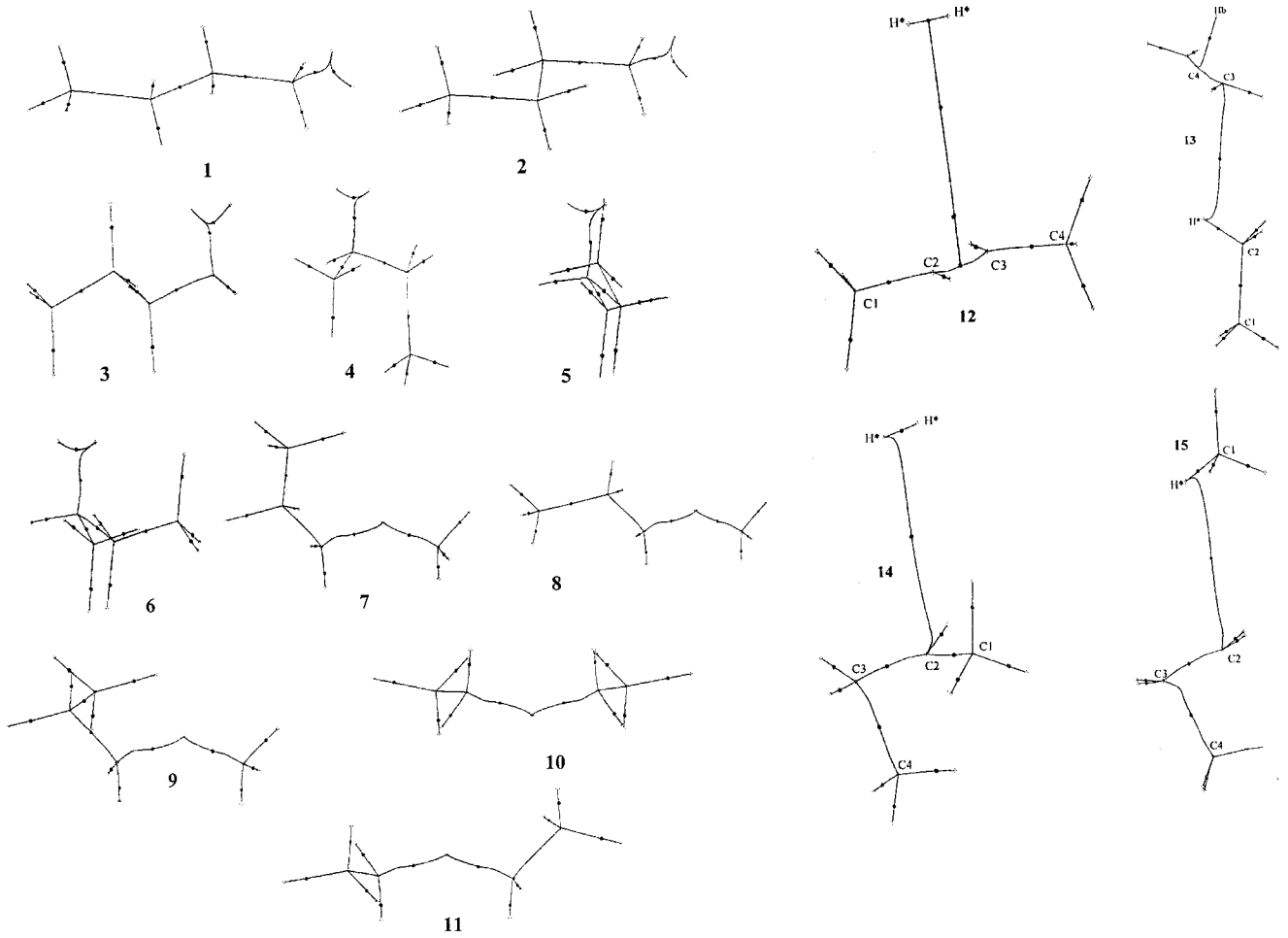

Figure 2. Molecular graphs corresponding to (a) species **1**−**11** and (b) species **12**−**15**.

SCHEME 3: Representation of the 3c−2e Bond in H-Carbonium and C-Carbonium Ions by Valence Bond (VB) Resonance Structures

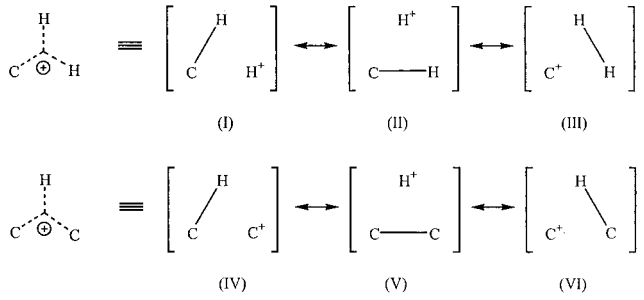

at the BCPs of structure **12**, corresponding to the interaction between the *s*-butyl cation and the hydrogen molecule. Bond distances are also included. It can be seen that the bond distance and the density, the Laplacian, and the ellipticity values are 1.490 Å and 0.2662 au, −0.7835, and 0.0367 au, for the C_1-C_2 and C_3-C_4 bonds, respectively. The bond distance C_2-C_3 is 1.393 Å, exhibiting the characteristics of a covalent double bond, where ρ_b has a relatively high value (0.3172 au); $\nabla^2\rho_b < 0$ (−0.9650 au) and $\epsilon = 0.2506$. It is interesting to note that, although the distance between the hydrogen denoted as H_b (bridged) and the C_2 and C_3 atoms is 1.301 Å, a single critical point is localized between these three atoms, indicating a 3c−2e bond in the $C_2H_5^+$ moiety. At this BCP, the density and Laplacian present relatively low values (0.1966 and −0.2783 au) and significant differences between the perpendicular curvatures ($\lambda_1 = -0.4191$ and $\lambda_2 = -0.1447$) can be seen.

As the ellipticity is derived from the relationship between the negative curvatures, its increase is a measure of how far the density distribution is distorted from the axial symmetry of the bond. ($\epsilon_{(C2-C3)} = 0.2506$ and $\epsilon_{(C3-Hb)} = 1.8958$). It would explain the π character of this 3c−2e bond formed between the bridged hydrogen atom and the C_2 and C_3 atoms.

The other two hydrogen atoms, denoted as H*−H*, show the characteristic of a shared interaction between them, where the bond distance is 0.736 Å, very similar from that of the H_2 isolated molecule. The remaining topological properties values in the H*−H* bond are also very similar.

In the complex **12**, the H_2 molecule is localized in a parallel plane from that formed by the carbon atoms, over a region of charge density accumulation between both secondary carbon atoms. It is about 2.36 Å away from the *sec*-butyl moiety. A single BCP is localized between both moieties, at 2.8029 and 0.9463 au from C_1 and H_b, respectively, showing characteristics of a closed shell interaction, ($\rho_b = 0.0071$ au and $\nabla^2\rho_b = 0.0204$ au). It can be also shown that the relationship $|\lambda_1|/\lambda_3 < 1$, (0.2024), as it generally is calculated for van der Waals interactions. Finally, although the ellipticity value in the H*−H* bond is nearly zero ($\epsilon = 0.0019$), a higher ellipticity value is found for the BCP that represent the interaction between both moieties ($\epsilon = 0.1384$ au).

Figure 4a shows the contour map of the Laplacian distribution $\nabla^2\rho$ for the van der Waals complex **12**, in the plane that contains the carbon atoms. The molecular graph is superimposed. As

TABLE 2: Topological Properties (in a.u.) of the Electronic Charge Density in 3c−2e BCP and Their Neighbor Bonds of 2-H-*n*-Butonium Cations (4−6; see Figure 1)[a]

		d(C−H*)	angle H*−C− H*	ρ_b	$\nabla^2\rho_b$	$\lvert\lambda_1\rvert/\lambda_3$	ϵ	G_b	V_b	G_b/ρ_b	V_b/G_b
4	C_2−H*	1.241	41.9	0.1994	−0.2407	2.2233	2.5662	0.1724	−0.4050	0.8646	2.3492
	C_2−H*	1.216									
5	C_2−H*	1.251	40.9	0.1937	−0.2455	1.8507	1.0293	0.1594	−0.3802	0.8229	2.3852
	C_2−H*	1.233									
6	C_2−H*	1.253	40.6	0.1915	−0.2232	1.7410	1.1098	0.1621	−0.3801	0.8465	2.3448
	C_2−H*	1.239									
6′	C_2−H*	1.290	37.7	0.1712	−0.0764	0.1535	2.4080	0.1699	−0.3590	0.9924	2.1130
	C_2−H*										
4	H*-H*	0.878		0.2257	−0.6604	2.4009	0.9218	0.0314	−0.2280	0.1391	7.2611
5		0.868		0.2258	−0.6815	2.0946	0.7227	0.0286	−0.2277	0.1267	7.9615
6		0.864		0.2269	−0.6928	2.0942	0.6940	0.0274	−0.2280	0.1208	8.3212
6′		0.832		0.2354	−0.7780	1.7911	0.4343	0.0208	−0.2362	0.0884	11.3558
4	$C-C_{Ethyl}$	1.567		0.2245	−0.5549	1.7587	0.0357	0.0644	−0.2675	0.2869	4.1537
5		1.532		0.2446	−0.6618	2.0335	0.0377	0.0710	−0.3075	0.2903	4.3310
6		1.536		0.2431	−0.6555	2.0059	0.0240	0.0702	−0.3043	0.2888	4.3348
4	$C-C_{Meth}$	1.517		0.2534	−0.7069	2.0578	0.0089	0.0681	−0.3129	0.2687	4.5947
5		1.520		0.2511	−0.6958	2.0570	0.0188	0.0686	−0.3111	0.2732	4.5350
6		1.520		0.2519	−0.6990	2.0496	0.0150	0.0683	−0.3113	0.2711	4.5578
4	C_2-H_o	1.096		0.2907	−1.0814	1.6320	0.0362	0.0316	−0.3336	0.1087	10.5570
5		1.100		0.2814	−1.0161	1.6158	0.0115	0.0344	−0.3229	0.1222	9.3866
6		1.099		0.2826	−1.0263	1.6152	0.0143	0.0336	−0.3237	0.1189	9.6339

[a] Also are included some relevant properties for 2-H-*iso*-butonium (**6′**). See the Method and Calculation Details section for an explanation of symbols. In all cases, (*) indicates the hydrogen atom involved in the 3c−2e bond and (0) indicates the hydrogen atom taken as reference. Bond distances in angstroms and angles in degrees are included.

can be see in Figure 4a, the H* atoms are projected over the plane that contains the central carbon atoms, in the region of the space where the electronic density is concentrated, corresponding to negative values of $\nabla^2\rho$. In this way, the hydrogen atoms are localized in an area of charge density concentration where a bonding interaction with the *sec*-butyl carbenium moiety takes place. Figure 4b shows the contour map of the Laplacian distribution for the same van der Waals complex **12** in a plane perpendicular to the previous one. It can be seen in Figure 4b that the bridged hydrogen atom is not located in the same plane defined by the network of carbon atoms but in a plane nearly perpendicular to it.

A region of charge accumulation (negative Laplacian values) is found over the $C_2-H_b-C_3$ atoms, whereas the bond trajectory between both moieties is found in a region of charge depletion, characteristic of a closed shell interaction.

Taking into account that structure **5**, corresponding to 2-H-*n*-butonium, proceeds to the formation of the van der Waals complex between the *s*-butyl cation and hydrogen (structure **12**), one can establish some comparisons between both structures. Tables 2 and 4 show the change in the charge density values of the bonds. In general, in **12**, the C−C bonds are shortened and the density on the BCPs increase, compared with those values corresponding to structure **5**. On the other hand, the corresponding H*−H* bond distance in structure **12** is 0.736 Å, shorter than in structure **5** (0.868 Å), and the density charge and Laplacian values are higher, whereas the ellipticipy value is lower than the corresponding values in structure **5** ($\rho_b = 0.2661$ au, $\nabla^2\rho_b = -1.1208$ au, $\epsilon = 0.0019$ in complex **12** and $\rho_b = 0.2258$ au, $\nabla^2\rho_b = -0.6815$ au, $\epsilon = 0.7227$ in **5**).

These results are very similar to those for the complex between the isopropyl cation and H_2, found in a previous work performed on the topological properties of proponium cations[19b] with the difference that, in this case, a 3c−2e bond is formed in the *s*-butyl cation moiety.

*van der Waals Complex **13**.* Table 5 shows the more significant topological local properties at the BCP's of structure **13** corresponding to the van der Waals complex between the ethyl cation ($C_2H_5^+$) and ethane, possibly formed from the decomposition of the 2-C-*n*-butonium cations. The ethyl cation has a bridged structure, in agreement with other experimental and theoretical results.[17] We have also included, in Table 5, the bond distances for comparison purposes.

The topological distribution of the electronic charge density in C−C bonds on the complex **13** shows clearly differences in both fragments. In the $C_2H_5^+$ cation, the C−C bond is involved in a 3c−2e bond, with the hydrogen atom bridged. The C−C bond distance is 1.382 Å, shorter than the corresponding distance in the ethane fragment (1.523 Å). The topological properties at the BCP in both C−C bonds are also different: $\rho_b = 0.3220$ au, $\nabla^2\rho_b = -1.0028$ au, and $\epsilon = 0.2404$ au and $\rho_b = 0.2518$ au, $\nabla^2\rho_b = -0.6754$ au, and $\epsilon = 0.000$ au, respectively. In the $C_2H_5^+$ fragment, the highest values of the curvatures λ_1 and λ_2, the ρ_b, $\nabla^2\rho_b$, and ϵ are indicative of a double bond character. Similarly, the C−H bonds of the C_2H_6 moiety, have density and Laplacian values of $\rho_b = 0.284$ au and $\nabla^2\rho_b = -1.030$ au, corresponding to the values found in the ethane molecule. It has to be pointed out that the C−H bond nearest to the $C_2H_5^+$ moiety shows a slight lengthening, associated with a decrease of ρ_b and $\nabla^2\rho_b$ values.

On the other hand, the C−H bonds lengths in $C_2H_5^+$ are 1.082 Å, the density values vary from 0.2998 to 0.2971 au, and the Laplacian valuse vary from −1.1839 to −1.1559 au. These high values clearly show the nature of this fragment with a hydrogen atom bridged between two carbon atoms in sp^2 hybridization. In particular, the values of the topological properties in the $C-H_b$ show that the hydrogen atom, H_b, is asymmetrically bonded to the carbon atoms in the $C_2H_5^+$ moiety, because of the interaction with the ethane molecule. ($\rho_b = 0.1975$ au, $\nabla^2\rho_b = -0.3148$ au, and $\epsilon = 1.3896$). This ϵ value is the highest from all of the BCPs on the van der Waals complex **13**.

In the structure **13**, both moieties are connected by H*; nevertheless, the topological properties of the two bonds involved in $C_{(C2H6)}$-H*-$C_{(C2H5+)}$ are very different. In fact, the

TABLE 3: Topological Properties (in a.u.) of the Electronic Charge Density in 3c−2e BCP and Their Neighbor Bonds of C−H-*n*-Butonium Cations (7−11; see Figure 1)[a]

		d(C−H*)	d(C−C)	angle C−H*−C	ρ_b	$\nabla^2\rho_b$	$\lvert\lambda_1\rvert/\lambda_3$	ϵ	G_b	V_b	G_b/ρ_b	V_b/G_b
7	C_1−H*	1.186	2.128	119.3	0.1908	−0.4402	1.7766	0.1731	0.0877	−0.2855	0.4596	3.2554
	C_2−H*	1.279			0.1413	−0.1565	0.8924	0.1419	0.0784	−0.1960	0.5548	2.5013
8	C_1−H*	1.189	2.131	119.8	0.1893	−0.4324	1.7363	0.1584	0.0871	−0.2823	0.4601	3.2411
	C_2−H*	1.275			0.1423	−0.1651	0.9206	0.1459	0.0788	−0.1989	0.5538	2.5241
9	C_1−H*	1.189	2.138	120.4	0.1890	−0.4309	1.7282	0.1372	0.0874	−0.2826	0.4624	3.2334
	C_2−H*	1.275			0.1420	−0.1619	0.9101	0.1633	0.0786	−0.1976	0.5535	2.5140
10	C_2−H*	1.231	2.222	129.4	0.1610	−0.2642	1.1877	0.1218	0.0848	−0.2356	0.5267	2.7783
	C_3−H*	1.227			0.1632	−0.2806	1.2417	0.0980	0.0858	−0.2417	0.5257	2.8170
11	C_2−H*	1.230	2.197	126.5	0.1630	−0.2731	1.2169	0.1546	0.0847	−0.2377	0.5196	2.8064
	C_3−H*	1.230			0.1632	−0.2742	1.2196	0.1484	0.0848	−0.2381	0.5196	2.8031
11′	C_1−H*	1.1370	2.470	142.3	0.2250	−0.6678	2.0403	0.0082	0.0763	−0.3195	0.3391	4.1874
	C_2−H*	1.4700			0.0786	0.0654	0.4037	0.2171	0.0499	−0.0834	0.6349	1.6713
7	C_1−H	1.080			0.2960	−1.1266	1.6580	0.0292	0.0296	−0.3408	0.1000	11.5135
	C_2−H	1.082			0.3004	−1.1624	1.6654	0.0393	0.0266	−0.3439	0.0885	12.9286
8	C_1−H	1.080			0.2961	−1.1280	1.6587	0.0294	0.0295	−0.3411	0.0996	11.5627
	C_2−H	1.082			0.3002	−1.1599	1.6690	0.0406	0.0270	−0.3441	0.0899	12.7444
9	C_1−H	1.080			0.2962	−1.1283	1.6605	0.0295	0.0297	−0.3414	0.1003	11.4949
	C_2−H	1.082			0.2999	−1.1578	1.6663	0.0397	0.0270	−0.3434	0.0900	12.7185
10	C_2−H_o	1.083			0.2987	−1.1452	1.6717	0.0351	0.0285	−0.3432	0.0954	12.0421
	C_1−H_o	1.086			0.2864	−1.0441	1.7243	0.0196	0.0386	−0.3382	0.1348	8.7617
	C_3−H_o	1.083			0.2986	−1.1435	1.6747	0.0349	0.0288	−0.3434	0.0965	11.9236
	C_4−H_o	1.085			0.2877	−1.0538	1.7121	0.0189	0.0376	−0.3386	0.1307	9.0053
11	C_2−H_o	1.082			0.2989	−1.1446	1.6729	0.0349	0.0288	−0.3438	0.0964	11.9375
	C_1−H_o	1.086			0.2865	−1.0445	1.7246	0.0197	0.0387	−0.3384	0.1351	8.7442
	C_3−H_o	1.082			0.2989	−1.1449	1.6738	0.0349	0.0289	−0.3440	0.0967	11.9031
	C_4−H_o	1.086			0.2864	−1.0442	1.7241	0.0197	0.0387	−0.3384	0.1351	8.7442
7	C_2−C_3			0.2615	−0.7568	2.3267	0.0335	0.0794	−0.3480	0.3036	4.3829	0.2615
	C_3−C_4			0.2549	−0.6921	1.7908	0.0107	0.0551	−0.2833	0.2162	5.1416	0.2549
8	C_2−C_3			0.2599	−0.7506	2.2956	0.0180	0.0786	−0.3449	0.3024	4.3880	0.2599
	C_3−C_4			0.2428	−0.6285	1.6811	0.0062	0.0543	−0.2657	0.2236	4.8932	0.2428
9	C_1−C_2			0.2598	−0.7463	2.2923	0.0373	0.0787	−0.3440	0.3029	4.3710	0.2598
	C_3−C_4			0.2547	−0.6914	1.7907	0.0110	0.0552	−0.2832	0.2167	5.1304	0.2547
10	C_1−C_2			0.2647	−0.7689	2.1982	0.0152	0.0713	−0.3349	0.2694	4.6971	0.2647
	C_3−C_4			0.2600	−0.7412	2.1223	0.0197	0.0701	−0.3256	0.2696	4.6448	0.2600
11	C_1−C_2			0.2646	−0.7688	2.2072	0.0150	0.0716	−0.3354	0.2706	4.6843	0.2646
	C_3−C_4			0.2644	−0.7680	2.2049	0.0149	0.0715	−0.3350	0.2704	4.6853	0.2644

[a] Also are included some relevant properties). See Method and Calculation Details sectionfor an explanation of symbols and Figure 1. In all cases, (*) indicates the hydrogen atom involved in the 3c−2e bond and (0) indicates the hydrogen atom taken as reference. Bond distances in angstroms and angles in degrees are included.

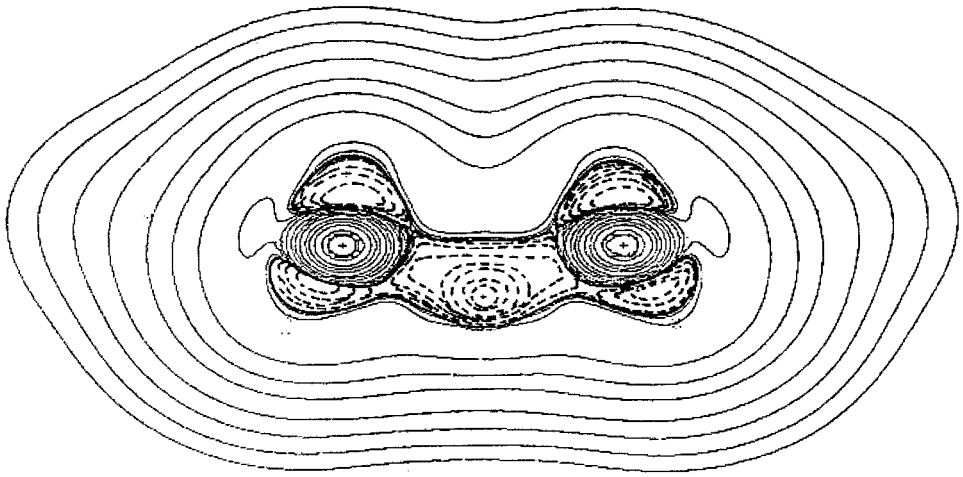

Figure 3. Contour map of the Laplacian distribution of the electronic charge density $\nabla^2\rho$ of structure **11** in the plane that contains the 3c−2e bond (C−H*−C). Solid lines represent regions of electronic charge depletion, and broken lines denote regions of electronic charge concentration.

density in the $C_{(C2H6)}$−H* BCP, is higher than the density in the corresponding $C_{(C2H5+)}$−H* BCP. The first BCP exhibits the characteristic of a covalent bond interaction, where ρ_b takes a value of 0.2767 au, and $\nabla^2\rho_b$ is negative, (−0.9837 au). It is also proved, in these cases, that the relationship, $|\lambda_1|/\lambda_3 > 1$, (1.8876) as it is generally found for covalent bond interactions. In the case of the $C_{(C2H5+)}$−H* bond, ρ_b and $\nabla^2\rho_b$ values are lower, indicating a weaker interaction: (0.0073 and 0.0294 au, respectively), with $|\lambda_1|/\lambda_3 < 1$ (0.1105), characteristic of a closed shell interaction. In this BCP, the elllipticity value found is $\epsilon = 0.9933$ showing a behavior similar to that described above.

TABLE 4: Topological Properties (in a.u.) of the Electronic Charge Density in the BCPs of the van der Waals Complex 12[a]

bond	distance	ρ_b	$\nabla^2\rho_b$	λ_1	λ_2	λ_3	$\lvert\lambda_1\rvert/\lambda_3$	ϵ
C_1-C_2	1.490	0.2662	−0.7835	−0.561	−0.4884	0.2108	2.4008	0.0367
C_2-C_3	1.393	0.3172	−0.9650	−0.6683	−0.5343	0.2377	2.8115	0.2506
C_3-C_4	1.490	0.2662	−0.7835	−0.5061	−0.4882	0.2108	2.4008	0.0367
C_2-H	1.087	0.2961	−1.1337	−0.8304	−0.8123	0.5089	1.6317	0.0223
C_3-H	1.087	0.2961	−1.1337	−0.8304	−0.8123	0.5089	1.6317	0.0223
C_3-H_b	1.301	0.1966	−0.2783	−0.4191	−0.1447	0.2855	1.4679	1.8958
C_1-H	1.086	0.2862	−1.0443	−0.7532	−0.7383	0.4472	1.6842	0.0203
C_1-H	1.085	0.2868	−1.0474	−0.7495	−0.7359	0.4380	1.7112	0.0185
C_1-H	1.091	0.2811	−1.0104	−0.7300	−0.7205	0.4400	1.6591	0.0132
C_4-H	1.086	0.2862	−1.0443	−0.7532	−0.7383	0.4472	1.6842	0.0203
C_4-H	1.091	0.2811	−1.0105	−0.7300	−0.7205	0.4400	1.6591	0.0132
C_4-H	1.085	0.2868	−1.0474	−0.7495	−0.7359	0.4380	1.7112	0.0185
s-butyl−H_2		0.0071	0.0204	−0.0067	−0.0059	0.0331	0.2024	0.1384
H*−H*	0.736	0.2661	−1.1208	−0.9055	−0.9038	0.6886	1.3150	0.0019

[a] See Method and Calculation Details section for an explanation of symbols and Figure 1. Bond distances in angstroms are included. In all cases, (*) indicates the hydrogen atom involved in the 3c−2e bond. H_b denotes the hydrogen atom bridged.

*van der Waals Complexes **14** and **15***. Tables 6 and 7 show the more significant topological local properties at the BCP's of **14** and **15** complexes, respectively.

The van der Waals complex **14** corresponds to the protonated methylcyclopropane and H_2, formed from the decomposition of the 2-H-*n*-butonium cations with anchimeric assistance from the methyl group at the β position relative to the 3c−2e bond.[12]

From the structural point of view, the protonated methylcyclopropane is similar to the one formed for the corner-protoned cyclopropane.[24]

The topology of the charge density in complex **14** shows only three BCPs between C−C bonds. One of them, corresponding to the C_1-C_{Met} bond, has a bond distance of 1.479 Å and shows different ρ_b and $\nabla^2\rho_b$ values from the others. The C_1-C_2 bond distance is 1.404 Å and $\rho_b = 0.3137$ au, $\nabla^2\rho_b =$ -0.9959 au, and $\epsilon = 0.1600$ au. On the other hand, the C_2-C_3 bond distance is 1.646 Å ($\rho_b = 0.1841$ au, $\nabla^2\rho_b = -0.3230$ au, and $\epsilon = 0.3523$ au) and does not exist BCP between the C_1 and C_3 atoms. No ring critical point is found as was expected, based in its similarity with the cyclopropane molecule.

As it can be seen in the molecular graph (Figure 2b) and in Table 6, the C_3-H_c bond ($d = 1.098$ Å), where H_c denotes the hydrogen atom at the corner of the cycle synclinal to the C_1-C_2 bond, shows charge density and Laplacian values slightly lower that those at the other C_3-H bonds ($\rho_b = 0.2745$ and $\nabla^2\rho_b = -0.9589$).

In addition, the properties at the H*−H* BCP are indicative of a shared interaction with a similar behavior to that on the H_2 isolated molecule.

Structure **15** represents the van der Waals complex between the CH_4 molecule and the protonated cyclopropane. Furthermore, it is important to point out that the behavior of the topological distribution of the charge density in this complex do not show a ring critical point in the later moiety.

In Table 7, it can be seen that the C−H bonds corresponding to the CH_4 fragment show bond distances, electronic charge density, and Laplacian values comparable to the isolated CH_4 molecule. Furthermore, the topological local properties at the $C_{(C3H7+)}-H^*$ bond show a closed shell interaction characterized by low density and Laplacian values. A positive Laplacian value is indicative of a depletion of the charge density. The atomic distance of C_1 to H* (methyl fragment) is 2.852 Å. The topological characteristics in this van der Waals interaction are given for the curvature λ_2 value. As it can be seen in the molecular graph of the complex **15** (Figure 2b and Table 7), the C_3-H_c bond shows a similar behavior of that corresponding bond in **14** with $d = 1.103$ Å, $\rho_b = 0.2691$ au, and $\nabla^2\rho_b =$ -0.9257 au.

From the topological charge density point of the view, this complex can be described as a 1-propyl cation structure and CH_4 better than to a protoned cyclopropane cation and CH_4 molecule.

Comparative Analysis of the *n*-Butonium and Isobutonium Ions in the Light of the AIM Theory of Bader

We found that a better understanding on the relative stability of the *n*-butonium and isobutonium isomers is obtained when the topological properties at the BCPs in the 3c−2e bonds are considered.

The comparative analysis on the geometric and topological parameters at BCPs of the C−H* and H*−H* bonds in 1-H-*n*-butonium (structures **1**−**3**), 1-H-isobutonium (**3′**), 2-H-*n*-butonium (**4**−**6**), and 2-H-isobutonium (**6′**) cations (Tables 1 and 2) allow us to achieve the following conclusions.

A 3c−2e bond of C−H*−H* type is found in all of the H-butonium cations.

In the BCP at the C−H* bonds, the electronic density values, ρ_b, (0.2128, 0.2122, 0.2200, 0.2090, 0.1994, 0.1937, 0.1915, and 0.1712 au) and the Laplacian of the density, $\nabla^2\rho_b$, (−0.4145, −0.4070, −0.4744, −0.3783, −0.2407, −0.2455, −0.2232, and −0.0764 au) values show a decrease when the carbon atom changes from primary to secondary. Moreover, it can be easily shown that, because of the electronic distribution in the three-center two-electron bonds, the electronic density, ρ_b, and the Laplacian of the density, $\nabla^2\rho_b$, values at H*−H* bonds are increased (0.2195, 0.2197, 0.2204, 0.2200, 0.2257, 0.2258, 0.2269, and 0.2354 au and −0.5816, −0.5854, −0.5322, −0.6002, −0.6604, −0.6815, −0.6928, and −0.7780 au, respectively). From the ρ_b, $\nabla^2\rho_b$, and ϵ values at the C−H* and H*−H* bonds, it can be concluded that there is a significant charge delocalization over the atoms in the 3c−2e region.

The relationship between the potential energy density and the kinetic energy density, V_b/G_b, at the BCP in H*−H* bonds shows an increase from 5.77 in 1-H-*n*-butonium to 6.12 in 1-H-isobutonium and from 7.26−8.32 in 2-H-*n*-butonium to 11.35 in 2-H-isobutonium. The increase of this relationship between both energy densities is accompanied by a decrease of the kinetic energy density for electronic charge unit. These facts suggest that both parameters could be taken as an index of the relative stability of the H*−H* bond in the 3c−2e bonds.

The C-carbonium ions show 3c−2e bonds with topological characteristics well defined, as can be seen in Table 3. As it was mentioned, structures **7**−**9** are derived from protonation

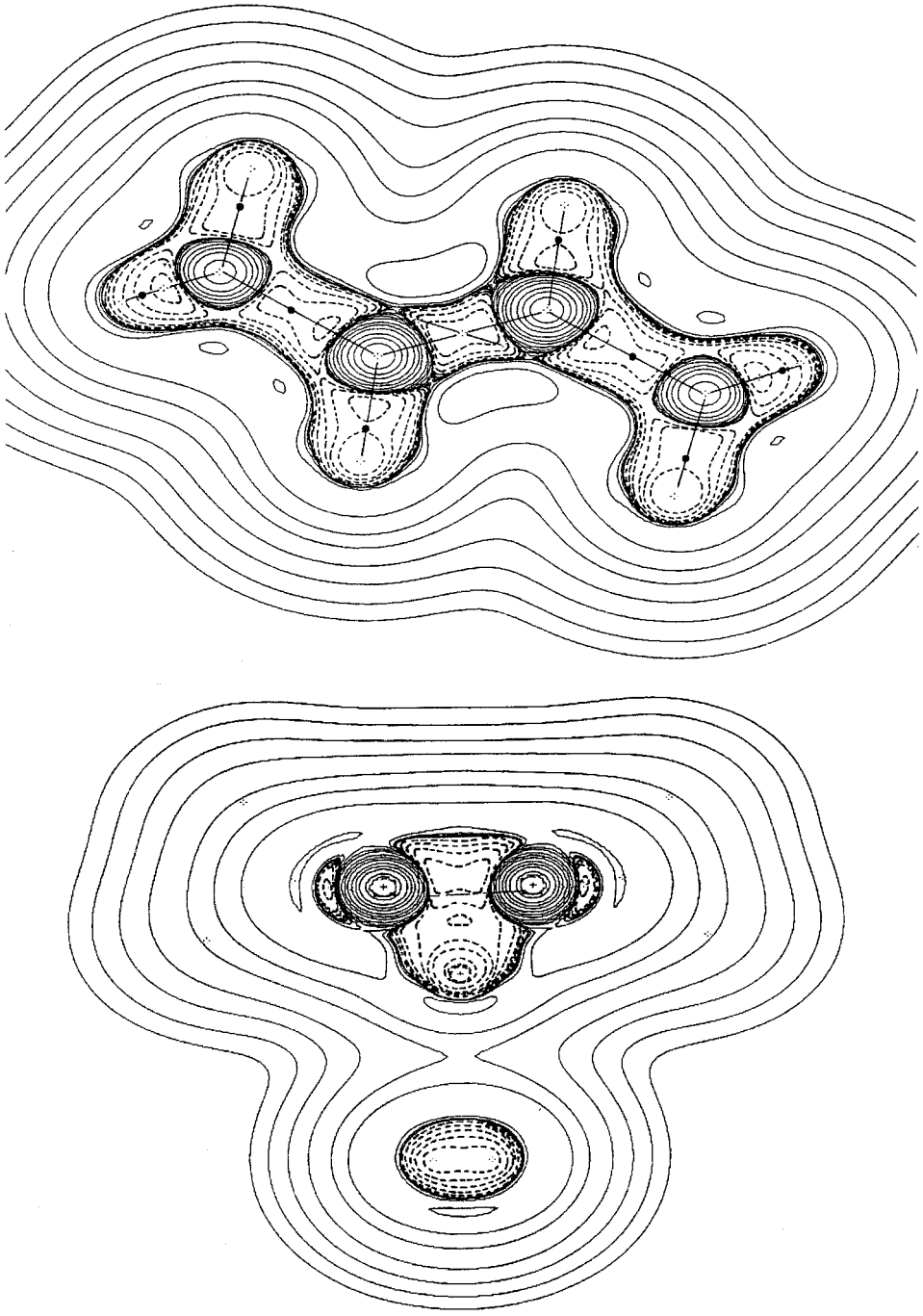

Figure 4. Laplacian of the electronic charge density $\nabla^2\rho$ of the van der Waals complex **12**. Solid lines represent regions of electronic charge depletion, and broken lines denote regions of electronic charge concentration. **(**a**)** Figure in the plane that contains the carbonated chain. The molecular graph is superimposed. Bond CPs are indicated with circles. **(**b**)** Figure in the plane perpendicular at the previous one and that contains the central carbon atoms and the H_2 moiety.

of the primary C−C bonds (external), corresponding to the 1-C-*n*-butonium ions, and protonation at the secondary C−C bond (internal) leads to the conformers **10** and **11** of the 2-C-*n*-butonium cations. On the other hand, C-isobutonium (**11′**) is formed upon protonation at the $C_{ter}-C_{prim}$ bond. From an inspection of the **7**-**9** structures, it can be seen that each one shows remarkable differences in the properties corresponding to the two C−H* bonds involved in the three center bonds: $C_{prim}-H^*-C_{sec}$. The density, the Laplacian of the density, the density of the kinetic and potential energies, and the V_b/G_b relationship are significant for the $C_{prim}-H^*$ bond, indicating a high bond order. These results are in agreement with previous calculations on C-proponium cations.[19b]

When structures **10** and **11** are considered, it has to be noted that they show the highest symmetry among all structures and similar structural and topological characteristics, particularly structure **11**, the more stable among all 15 structures. Thus, the two $C_{sec}-H^*$ bonds of the 3c−2e bonds as well as the neighbor C−C bonds have the same length and nearly similar topological properties, indicating that the charge of the cation is equally delocalized through the σ bonds of the carbon chain, which stabilizes the structure.

On the other hand, the charge delocalization over the atoms in the 3c−2e region in the C-isobutonium cation is more asymmetric than those of the other isomeric C-*n*-butonium cations. The electronic density at the two BCPs of the C−H*

TABLE 5: Topological Properties (in a.u.) of the Electronic Charge Density in the Bond Critical Points (3, −1) of the van der Waals Complex 13[a]

bond	distance, Å	ρ_b	$\nabla^2\rho_b$	λ_1	λ_2	λ_3	$\lvert\lambda_1\rvert/\lambda_3$	ϵ
$C-H^*_{(C2H6)}$	1.092	0.2767	−0.9837	−0.6699	−0.6687	0.3549	1.8876	0.0018
$C-H_{(C2H6)}$	1.090	0.2801	−1.0035	−0.6921	−0.6904	0.3789	1.8266	0.0025
$C-H_{(C2H6)}$	1.089	0.2810	−1.0085	−0.6982	−0.6966	0.3863	1.8074	0.0022
$C-H^*_{(C2H5+)}$	2.657	0.0073	0.0294	−0.0039	−0.0019	0.0353	0.1105	0.9933
$C-C_{(C2H6)}$	1.523	0.2518	−0.6754	−0.4751	−0.4750	−0.2747	1.7295	0.0000
$C-H_{(C2H6)}$	1.086	0.2846	−1.0307	−0.7252	−0.7162	0.4107	1.7658	0.0126
$C-H_{(C2H6)}$	1.086	0.2843	−1.0286	−0.7223	−0.7127	0.4063	1.7777	0.0134
$C-H_{(C2H6)}$	1.086	0.2843	−1.0291	−0.7227	−0.7133	0.4070	1.7757	0.0133
$C-C_{(C2H5+)}$	1.382	0.3220	−1.0028	−0.6799	−0.5481	0.2252	3.0191	0.2404
$C-H_{(C2H5+)}$	1.082	0.2998	−1.1839	−0.8717	−0.8519	0.5397	1.6151	0.0232
$C-H_{(C2H5+)}$	1.082	0.2992	−1.1785	−0.8674	−0.8476	0.5364	1.6171	0.0233
$C-H_{b(C2H5+)}$	1.335	0.1975	−0.3148	−0.4249	−0.1778	0.2879	1.4758	1.3896
$C-H_{(C2H5+)}$	1.082	0.2971	−1.1559	−0.8482	−0.8341	0.5264	1.6113	0.0168
$C-H_{(C2H5+)}$	1.082	0.2971	−1.1562	−0.8485	−0.8344	0.5267	1.6110	0.0168

[a] See Method and Calculation Details section for an explanation of symbols and Figure 1. Bond distances in angstroms are included. In all cases, (*) indicates the hydrogen atom involved in the 3c−2e bond and (0) indicates the hydrogen taken as reference. H_b denotes the hydrogen atom bridged.

TABLE 6: Topological Properties (in a.u.) of the Electronic Charge Density in the Bond Critical Points (3, −1) of the van der Waals Complex 14[a]

bond	distance, Å	ρ_b	$\nabla^2\rho_b$	λ_1	λ_2	λ_3	$\lvert\lambda_1\rvert/\lambda_3$	ϵ
C_1-C_{Met}	1.479	0.2738	−0.8277	−0.5253	−0.5054	0.2030	2.5877	0.0392
$C_{Met}-H$	1.086	0.2864	−1.0454	−0.7545	−0.7390	0.4481	1.6838	0.0211
$C_{Met}-H$	1.086	0.2867	−1.0475	−0.7517	−0.7374	0.4416	1.7022	0.0194
$C_{Met}-H$	1.094	0.2774	−0.9872	−0.7153	−0.7094	0.4374	1.6353	0.0083
C_1-C_2	1.404	0.3137	−0.9959	−0.6495	−0.5599	0.2134	3.0436	0.1600
C_2-C_3	1.646	0.1841	−0.3230	−0.3133	−0.2317	0.2418	1.2957	0.3523
C_1-H	1.085	0.3011	−1.1744	−0.8642	−0.8342	0.5239	1.6495	0.0360
C_2-H	1.080	0.2952	−1.1125	−0.8073	−0.7945	0.4892	1.6502	0.0161
C_2-H	1.081	0.2942	−1.1050	−0.8017	−0.7885	0.4852	1.6523	0.0168
C_3-H	1.082	0.2906	−1.0730	−0.7846	−0.7681	0.4797	1.6356	0.0215
C_3-H	1.084	0.2887	−1.0626	−0.7817	−0.7633	0.4825	1.6201	0.0241
C_3-H_c	1.098	0.2745	−0.9589	−0.6897	−0.6837	0.1446	1.6635	0.0087
C_1-H^*	3.254	0.0024	0.0092	−0.0014	−0.0007	0.0114	0.1228	0.8351
H^*-H^*	0.735	0.2667	−1.1258	−0.9097	−0.9092	0.6931	1.3125	0.0005

[a] See Method and Calculation Details section for an explanation of symbols and Figure 1. Bond distances in angstroms are included. In all cases, (*) indicates the hydrogen atom involved in the 3c−2e bond and (0) indicates the hydrogen taken as reference. H_c denotes the hydrogen atom at the corner of the cycle.

TABLE 7: Topological Properties (in a.u.) of the Electronic Charge Density in the Bond Critical Points (3, −1) of the van der Waals Complex 15

bond	distance, Å	ρ_b	$\nabla^2\rho_b$	λ_1	λ_2	λ_3	$\lvert\lambda_1\rvert/\lambda_3$	ϵ
C_2-C_3	1.677	0.1716	−0.2044	−0.2896	−0.1470	0.2322	1.2472	0.9692
C_1-C_2	1.395	0.3152	−0.9870	−0.6553	−0.5537	0.2220	2.9518	0.1833
C_3-H_c	1.103	0.2691	−0.9257	−0.6804	−0.6710	0.4257	1.5983	0.0140
C_3-H	1.082	0.2903	−1.0743	−0.7943	−0.7709	0.4909	1.6180	0.0304
C_3-H	1.082	0.2903	−1.0737	−0.7940	−0.7705	0.4908	1.6178	0.0305
$C_{1(sp2)}-H$	1.081	0.3000	−1.1706	−0.8601	−0.8364	0.5258	1.6358	0.0283
$C_{1(sp2)}-H$	1.081	0.3005	−1.1747	−0.8634	−0.8374	0.5285	1.6337	0.0282
$C_{2(sp2)}-H$	1.079	0.2969	−1.1315	−0.8251	−0.8101	0.5037	1.6381	0.0185
$C_{2(sp2)}-H$	1.079	0.2970	−1.1318	−0.8254	−0.8105	0.5042	1.6370	0.0184
C_1-H^*	2.852	0.0052	0.0213	−0.0026	−0.0001	0.0246	0.1057	2.9694
$C_{Met}-H$	1.087	0.2793	−0.9980	−0.6939	−0.6880	0.3839	1.8075	0.0086
$C_{Met}-H$	1.086	0.2807	−1.0056	−0.7042	−0.6986	0.3972	1.7729	0.0079
$C_{Met}-H^*$	1.087	0.2779	−0.9894	−0.6833	−0.6773	0.3712	1.8408	0.0088
$C_{Met}-H$	1.084	0.2834	−1.0226	−0.7271	−0.7264	0.4309	1.6834	0.0001

[a] See Method and Calculation Details section for an explanation of symbols and Figure 1. Bond distances in angstroms are included. In all cases, (*) indicates the hydrogen atom involved in the 3c−2e bond. H_c denotes the hydrogen atom at the corner of the cycle.

bonds is very different. In fact, the density at the BCP between hydrogen, H*, and carbon atom of the methyl group is greater that the density in the C−H* bond formed with the carbon atom of the isopropyl group. Both BCPs show very different topological characteristics in the function of the values that adopt the curvatures, and they allow us to characterize the first BCP as a shared interaction, where the $\nabla^2\rho_b$ is negative and the relationship between curvatures $|\lambda_1|/\lambda_3 > 1$, (2.0403) as it is generally found for covalent bond interactions. On the contrary, in the second BCP, the ρ_b is lower, $\nabla^2\rho_b$ is positive, and the relation $|\lambda_1|/\lambda_3$ is <1, (0.4037), as can be seen in a closed shell interaction. Indeed, the ellipticity value (0.2171) in the last case is greater than that in the other C−H bonds in methyl groups of the C-isobutonium cation or from the isobutane molecule.

It is important to point out that the behavior of the topological distribution of the charge density in the 3c−2e bonds shows a

dependence with the bond angle and with the distance between carbon atoms involved in the three center two electron bond (the bond angle ranging from 119.3° to 129.4°, over species **7**, **8**, **9**, and **10** and having the value of 142.3° in C-isobutonium cation, whereas in **11**, the three center bond angle is 126.5°). However, structure **11** in C-*n*-butonium cations is more stable than the isomer **10** because of the electron delocalization and the symmetry over all of the molecule. At the last, structures **11** and **11′** are the most stable species formed upon protonation at the C−C bond.

It can be said that the origin of the stabilization of the last reported structures is different. In structure **11′**, an H*−CH_3 bond is formed with high density between the bonded atoms (shared interactions), whereas an H*−C_3H_7 bond with low electron density and high ellipticity, (closed shell interaction) is formed. Moreover, electronic delocalization over the methyl groups in the isopropyl fragment is observed.

Conclusions and Perspectives

It can be observed that in all of the species analyzed the C−H* bonds are weaker than the C−H_0 bonds that do not participate in the 3c−2e bonds.

The topological analysis of the distribution of the charge density reveals that the stability of the protonated species depends fundamentally on the way in which the charge of the cation is delocalized around the 3c−2e bonds.

It was found that in the H-*n*-butonium cations the stability of the species increases as the properties of the H*−H* bond resemble that of the unperturbed H−H bond from the H_2 molecule, which points to a more stable carbenium ion interacting with the H_2 moiety. In the C-*n*-butonium cations, the stability of the species seems to be associated to higher stabilities of the carbon containing moieties (two primary carbenium ions in the case of the 2-C-*n*-butonium ion and a methyl and primary 1-propyl cation in the case of the 1-C-*n*-butonium cation, see Scheme 3).

Topological analysis of the H-butonium cations reveals that the stabilization degree of the protoned species is related with an increase of the electronic density between the H* atoms and with a decrease of the density between H* and C atoms involved in the three centers bond. This again express the higher stability of more substituted carbenium ion moiety in the resonance structures (Scheme 3).

We concluded that, as the bond order between the hydrogen atoms increase because of the increment of the density and the Laplacian values in the BCP in the H*−H* bond and the two negative curvatures resemble each other ($\lambda_1 \approx \lambda_2$), the protoned H-carbonium species becomes more stable. These findings are followed by a shortening of the H*−H* and a lengthening of the C−H* distances and the decreasing of the H*−C−H * angle.

The strong similarity between H-carbonium and C-carbonium cations lies in the redistribution of the electron density that accompanies their formation.

The analysis of the C-carbonium cations shows that more stable species result when the C−H*−C angle and C−C distance increase, as well as the delocalization of the electronic density on the atoms involved in the three centers bond and the remaining fragment (isopropyl fragment in **11′**).

Thus, the stability order is

$$C_{Tertiary} > C_{Secondary} > C_{Primary}$$

In all cases in that the protonation is carried out giving different fragments, the bond distance between H* atoms and the C atom of the methyl fragment is smaller, and the interaction is shared type and the electronic density in the BCP is higher on the primary carbon atom than on the remaining (secondary and tertiary) carbon atoms.

The calculated topological properties from structure **12** show that the C_2-C_3 bond exhibits the characteristic of a covalent double bond, whereas the other C−C bonds show a single covalent bond behavior. A BCP is found among the hydrogen denoted as H_b (bridged) and the C_2 and C_3 atoms indicating the existence of a 3c−2e bond with a markedly π character showed by its ellipticity value. The two hydrogen atoms, denoted as H*−H*, show the characteristic of a shared interaction between them as in the isolated H_2 molecule. In complex **12**, the H_2 molecule is localized in a parallel plane from that formed by the carbon atoms, over a region of charge density accumulation between both secondary carbon atoms. A single BCP is localized between both moieties (between C_1 and H_b) showing the characteristic of a closed shell interaction, as it generally happens in a van der Waals interaction. Finally, although the ellipticity value in the H_2 moiety is nearly zero, a considerable ellipticity value is found for the interaction between both moieties. This higer value is clearly indicative that this bond is near to be broken, and would explain the dissociation of the complex **12** into the *s*-butyl carbenium ion and the H_2 molecule.

In structure **13**, the topological distribution of the electronic charge density in C−C bonds shows clearly differences in both fragments. In the $C_2H_5^+$ cation, the C−C bond is involved in a 3c−2e bond, with the hydrogen atom bridged (H_b) with two carbon atoms in sp^2 hybridization. This H_b is asymmetrically bonded to the carbon atoms because of the interaction with the ethane molecule. The topological properties are indicative of a double character bond in C−C. On the other hand, the topological bond properties of the C_2H_6 moiety are similar to those corresponding to the ethane.

The topology of the charge density in complex **14** shows only three BCP between C−C bonds, and no ring critical point is found as it would be expected because of their similarity with the methyl cyclopropane molecule. In addition, the properties at the H*−H* BCP are indicative of a shared interaction with a similar behavior to the that on the H_2 isolated molecule.

It is important to point out that, contrary to expectation, structure **15** does not show a ring critical point. Thus, from the topological charge density point of view, structure **15** is more similar to a van der Waals complex between a primary 1-propyl cation and a CH_4 molecule than to a van der Waals complex between a protoned cyclopropane cation and a CH_4 molecule.

Finally, it was seen that the study of the topology of the charge density is a powerful tool for exploring the stability and origin of the different structures formed in hydrocarbon protonation processes.

References and Notes

(1) (a) Olah, G. A.; Schlosberg, R. H. *J. Am. Chem. Soc.* **1968**, *90*, 2726. (b) Olah, G. A.; Prakash, G. K. S.; Williams, R. E.; Field, L. D.; Wade, K. *Hypercarbon Chemistry*; Wiley: New York, 1987.

(2) Olah, G. A.; Klopman, G.; Schlosberg, R. H. *J. Am. Chem. Soc.* **1969**, *91*, 3261.

(3) Hogeveen, H.; Bickel, A. F. *Recl. Trav. Chim. Pays-Bas.* **1969**, *88*, 371.

(4) Schleyer, P. v. R.; Carneiro, J. W. M. *J. Comput. Chem.* **1992**, *13*, 997−1003.

(5) Olah, G. A.; Rasul, G. *Acc. Chem. Res.* **1997**, *30*, 245−250.

(6) Schreiner, P. R.; Kim, S. J.; Schaefer, H. F.; Schleyer, P. V. R. *J. Chem. Phys*. **1993**, *99*, 3716.

(7) Marx, D.; Parrinello, M. *Nature* **1995**, *375*, 216.

(8) Carneiro, J. W. M.; Schleyer, P. V. R.; Saunders, M.; Remington, R.; Schaefer, H. F., III.; Rauk, A.; Sorensen, T. S. *J. Am. Chem. Soc.* **1994**, *116*, 3483−3493.

(9) Esteves, P. M.; Mota, C. J. A.; Ramirez-Solis, A.; Hernandez-Lamoneda, R. J. *J. Am. Chem. Soc.* **1998**, *120*, 3213.

(10) Mota, C. J. A.; Esteves, P. M.; Ramirez-Solis, A.; Hernandez-Lamoneda, R. *J. Am. Chem. Soc.* **1997**, *119*, 5193−5199.

(11) Esteves, P. M.; Mota, C. J. A.; Ramirez-Solis, A.; Hernandez-Lamoneda, R. *J. Top. Catal*. **1998**, *6*, 163−168.

(12) Esteves, P. M.; Alberto, G. G. P.; Ramirez-Solis, A.; Mota, C. J. A. *J. Phys. Chem. A* **2000**, *104*, 6233−6240.

(13) (a) Olah, G. A.; Halpern, Y.; Schen, J.; Mo, Y. K *J. Am. Chem. Soc*. **1973**, *95*, 4960. (b) Olah, G. A. *Angew. Chem., Int. Ed. Engl*. **1973**, *12*, 171. (c) Olah, G. A.; Prakash, G. K. S.; Williams, R. E.; Field, L. D.; Waade, K. *Hypercarbon Chemistry*; Wiley: New York, 1987.

(14) (a) Esteves, P. M.; Ramirez-Solis, A.; Mota, C. J. A. *J. Braz. Chem. Soc*. **2000**, *11*, 345 (available at http://www.sbq.org.br/jbcs/). (b) Esteves, P. M.; Ramírez-Solís, A.; Mota, C. J. A. *J. Phys. Chem. B* **2001**, *105*, 4331−4336. (c) Esteves, P. M.; Alberto, G. G. P.; Ramirez-Solis, A.; Mota, C. J. A. *J. Am. Chem. Soc.* **1999**, *121*, 7345.

(15) Bader, R. F. W. *Atoms in Molecules. A Quantum Theory*; Clarendon: Oxford, U.K., 1990.

(16) Popelier, P. L. A. *Atoms in Molecules. An Introduction*; Pearson Education: Harlow, U.K., 1999.

(17) Sieber, S.; Buzek, P.; Schleyer, P. v. R.; Kock, W.; Carneiro, J. W. M. *J. Am. Chem. Soc*. **1993**, *115*, 259.

(18) (a) Raghavachari, K.; Whiteside, R. A.; Pople, J. A. Schleyer, P. v. R. *J. Am. Chem. Soc*. **1981**, *103*, 5649. (b) Carneiro, J. W. M.; Schleyer, P. v. R.; Saunders, M.; Remington, R.; Schaefer, H. F., III.; Rauk, A.; Sorensen, T. S. *J. Am. Chem. Soc*. **1994**, *116*, 3483. (c) Hiraoka, K.; Mori, T.; Yamabe, S. *Chem. Phys. Lett*. **1993**, *207*, 178.

(19) (a) Okulik, N.; Peruchena, M.; Esteves, P. M.; Mota, C.; Jubert, A. H. *J. Phys. Chem. A*. **1999**, *103*, 8491. (b) Okulik, N.; Peruchena, M.; Esteves, P. M.; Mota, C.; Jubert, A. H. *J. Phys. Chem. A*. **2000**, *104*, 7586.

(20) Frisch, M. J.; Trucks, G. W.; Schlegel, H. B.; Gill, P. M. W.; Johnson, B. G.; Robb, M. A.; Cheeseman, J. R.; Keith, T.; Petersson, G. A.; Montgomery, J. A.; Raghavachari, K.; Al-Laham, M. A.; Zakrzewski, V. G.; Ortiz, J. V.; Foresman, J. B.; Cioslowski, J.; Stefanov, B. B.; Nanayakkara, A.; Challacombe, M.; Peng, C. Y.; Ayala, P. Y.; Chen, W.; Wong, M. W.; Andres, J. L.; Replogle, E. S.; Gomperts, R.; Martin, R. L.; Fox, D. J.; Binkley, J. S.; Defrees, D. J.; Baker, J.; Stewart, J. P.; Head-Gordon, M.; Gonzalez, C.; Pople, J. A. *Gaussian 94*, revision E.1; Gaussian, Inc.: Pittsburgh, PA, 1995.

(21) Klieger-Konig, W.; Bader, R. F. W.; Tag, T. H. *J. Comput. Chem.* **1982**, *3*, 317.

(22) Olah, G. A. *J. Am. Chem. Soc*. **1972**, *94*, 807.

(23) Pallis, J.; Male, S. *Pure Math*. **1970**, *14*, 223.

(24) Kock, W.; Liu, B.; Schleyer, P. v. R. *J Am. Chem. Soc*. **1989**, *11*, 3479.